JOURNAL OF MATERIALS SCIENCE 21 (1986) 3817–3822

Rigid body translation in the $(\bar{2}11)$ twin boundary in silicon

Ph. KOMNINOU, Th. KARAKOSTAS
Physics Department, University of Thessaloniki, Thessaloniki, Greece
P. DELAVIGNETTE
Materials Physics Department, CEN/SCK, Boeretang 200, B-2400 Mol, Belgium

The rigid body translation accompanying a $(\bar{2}\,1\,1)$ twin boundary in silicon has been studied by transmission electron microscopy. From a detailed analysis of the α-type fringe systems in the 1 1 1, 3 1 1 and 2 $\bar{2}$ 0 common reflections, the following translation vector is deduced: $\frac{1}{5}[0\,1\,1]$, which is equivalent to $\frac{1}{15}[4\,1\,1]$ in the other crystal element. A slight deviation of this orientation is possible.

1. Introduction

The rigid body translation in the non-coherent $(\bar{2}\,1\,1)$ twin plane of silicon has been repeatedly examined [1–8], and different models of the atomic arrangement have been proposed [2, 3, 7, 8]. The presence of α-type fringes in transmission electron microscopy (TEM) images for particular reflections indicate that, in contrast with the (1 1 1) twin plane (for which no translation is observed), the displacement shift complete (DSC) lattice referred to atomic positions is not continuous through the $(\bar{2}\,1\,1)$ twin plane, but is shifted of a translation, $\boldsymbol{R}$, which is not a DSC lattice vector [1, 2, 7, 8]. A vector $\boldsymbol{R} = \frac{1}{4}[0\,1\,1]$ has been proposed, and evidence of a small deviation from that vector is occasionally suggested [2]. Other authors mention a determination of the rigid body translation based on the contrast of α-fringes without presenting more detailed information [8].

Atomic configurations based on energetic calculations have been proposed and models have been compared with experimental results [2, 8]. The characteristics of the observed contrast as well as its great variability impeded a clear determination of the rigid body translation. They will be studied below. There is a certain consensus to suggest a translation close to $\frac{1}{4}[0\,1\,1]$. In the same $(\bar{2}\,1\,1)$ boundary plane, two different translations have been observed [2]. Electron diffraction indicates the presence in the boundary plane of a periodicity of $[0\,1\,\bar{1}]$, while in each crystal part the periodicity is $\frac{1}{2}[0\,1\,1]$ [5–7]. High resolution electron microscopy does not allow a definitive determination of atomic arrangements in the boundary plane [7].

2. Experimental techniques

As-received polycrystalline silicon wafers for solar cell applications from directionally solidified ingots (p-type), resistivity 10^{-2} to 10^{-4} ohm m^{-1} were chemically thinned to electron transparency. The solvent was 9 parts HNO_3 : 1 part HF. Occasionally a final ion thinning of a few hours was performed. The specimens were examined using a Jeol 200 CX transmission electron microscope operated at an acceleration voltage of 200 kV.

3. The rigid body translation

If an atomic lattice is continuous through a twin boundary, in every transmission electron microscope (TEM) image taken with a reflection which is common to both crystal grains, the twin boundary will be invisible. On the other hand, if some of these reflections show an α-type fringe system, this reveals the presence of a rigid body translation, $\boldsymbol{R}$, that is not a DSC lattice vector. This translation is a multivalued function; all vectors joining the DSC lattice points to a point $R(u, v, w)$ in that unit cell are equally valid descriptions of the translation.

In TEM observations, two reflections for which no contrast (or a typical $\alpha = 180°$ fringe contrast) is observed, allow a determination of a segment or of segments in the unit cell on which the point $R(u, v, w)$ is possibly situated. The smallest $\boldsymbol{R}$ vector will be generally preferred for the description of the rigid body translation.

In the case of the twin in silicon, the DSC lattice is based on the following hexagonal unit cell: $\frac{1}{6}[\bar{2}\,1\,1]$, $\frac{1}{6}[1\,\bar{2}\,1]$, $\frac{1}{3}[1\,1\,1]$. The observed twin plane in polycrystalline silicon is generally the coherent (1 1 1) twin plane. This plane is always free of a rigid body translation (no α-fringes in common reflections). More rarely faceted twin boundaries are observed in the (1 1 1) and $(\bar{2}\,1\,1)$ planes. The facets in the $(\bar{2}\,1\,1)$ plane present α-fringe systems in some common reflections, revealing the presence of a rigid body translation. Actually two possible translations are observed in different $(\bar{2}\,1\,1)$ facets, $\boldsymbol{R}_1$ and $\boldsymbol{R}_2$. They will be analysed later. A dislocation is present along the intersection line between a (1 1 1) and a $(\bar{2}\,1\,1)$ facet, and its Burgers vector is a possible $\boldsymbol{R}$ vector.

4. Observation of α-fringes

The $(\bar{2}\,1\,1)$ twin boundary is examined in all possible common reflections. They correspond to the 24 planes perpendicular to the common rotation axes

0022–2461/86 $03.00 + .12

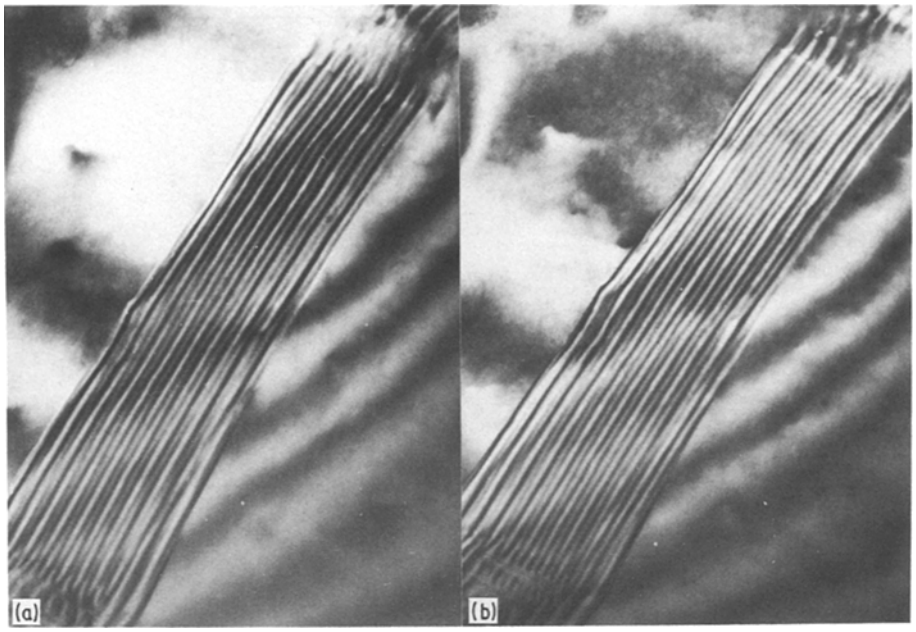

Figure 1 Facet in a $(\bar{2}\,1\,1)$ plane of a twin boundary in silicon as observed in the 1 1 1 reflection and showing a dedoubled fringe system typical of a high α value. (a) bright field in 1 1 1, (b) dark field in $\bar{1}\,\bar{1}\,\bar{1}$.

describing the twin. The observed contrast types are subdivided in three categories. In reflections like $0\,2\,\bar{2}$, $3\,1\,\bar{1}$ and $3\,\bar{1}\,1$, the twin boundary is invisible, indicating a rigid body translation $\boldsymbol{R}_1$ for which $\boldsymbol{g} \cdot \boldsymbol{R}_1 = N$, where N is an integer or 0 ($\alpha = 2\pi \boldsymbol{g} \cdot \boldsymbol{R} = 0 \bmod 2\pi$). In reflections like 1 1 1, $2\,\bar{2}\,0$ and $2\,0\,\bar{2}$, a strong α-type fringe contrast is observed (Figs 1 and 2) for which the fringe periodicity is given by an increase in crystal thickness of $\xi_g/2$, typical for a fringe system where $\alpha = 180°$ or N is an integer plus $\frac{1}{2}$. In reflections like $\bar{1}\,1\,3$, $\bar{1}\,3\,1$, weaker α-type fringe systems are observed (Fig. 3) with generally a periodicity of ξ_g typical for $\alpha \neq 0$, $\neq 180°$ and for a "thick" crystal. The facets characterized by the translation vector $\boldsymbol{R}_2$ show an α-fringe system for the reflections $3\,1\,\bar{1}$ and $3\,\bar{1}\,1$ and an extinction in the reflections $\bar{1}\,1\,3$ and $\bar{1}\,3\,1$. All Miller indices are referred to one element of the twin called grain A.

The extinctions indicate a possible translation vector $\boldsymbol{R}_1 = 1/n\ [0\,1\,1]$ and assimilating the 1 1 1 contrast to an $\alpha = 180°$ type, a vector $\boldsymbol{R}_1 = \frac{1}{4}[0\,1\,1]$ is deduced. Although this is in contradiction with the $\{3\,1\,1\}$ type contrasts, it will be chosen as a first approximation from which a closer analysis of the α-type fringe system will allow the determination of a small deviation of that vector.

5. Possible rigid body translation

Different deviations from $\frac{1}{4}[0\,1\,1]$ will be examined successively: a pure shear along $[0\,1\,\bar{1}]$, a pure shear along $[1\,1\,1]$ and a pure dilatation along $[\bar{2}\,1\,1]$. Table I summarizes the characteristics of α-type fringes for different reflections and different translation vectors. If $\boldsymbol{g} \cdot \boldsymbol{R}_1$ is 0 or an integer, $\alpha = 0$ and the boundary is invisible; if $\boldsymbol{g} \cdot \boldsymbol{R}_1 = \frac{1}{2}$ then $\alpha = 180°$.

The first line presents the contrast for $\boldsymbol{R}_1 = \frac{1}{4}[0\,1\,1]$. It is not a correct vector since it predicts an extinction for the four 3 1 1 reflections. A pure shear of a small magnitude $\varepsilon[0\,1\,\bar{1}]$ results in the contrast given by the second line; this contradicts the observation of the four 3 1 1 reflections for which four times the same type of contrast is predicted. The same conclusion is

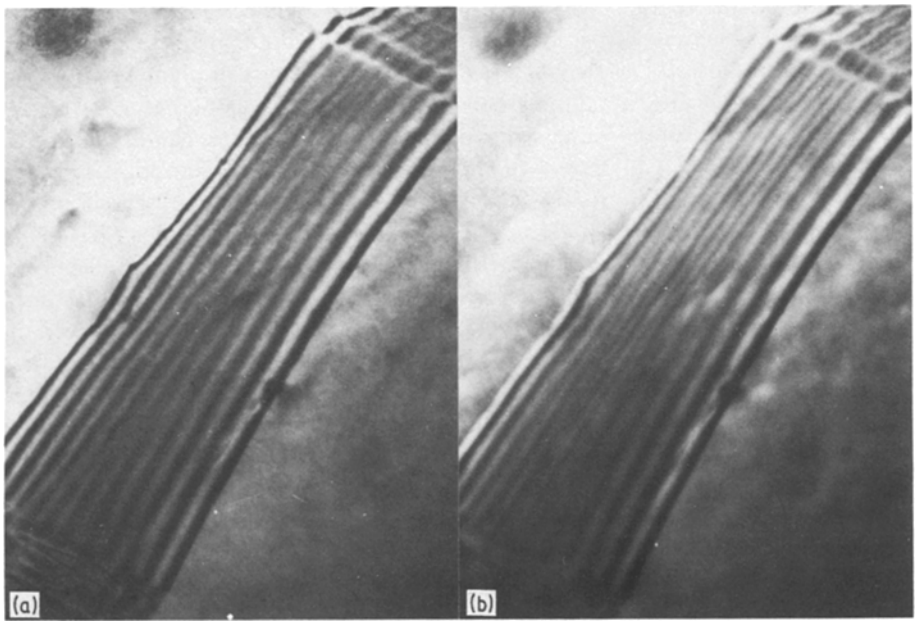

Figure 2 Same twin boundary as in Fig. 1 observed in the $2\,0\,\bar{2}$ reflection. (a) bright field in $2\,0\,\bar{2}$, (b) dark field in $\bar{2}\,0\,2$.

TABLE I Values of $g \cdot R$ for different rigid body translations and different reflections

$g \cdot R_I$	1 1 1	2 $\bar{2}$ 0	2 0 $\bar{2}$	$\bar{1}$ 1 3	$\bar{1}$ 3 1	0 2 $\bar{2}$	3 1 $\bar{1}$	3 $\bar{1}$ 1
$\frac{1}{4}$[0 1 1]	$\frac{1}{2}$	$-\frac{1}{2}$	$-\frac{1}{2}$	1	1	0	0	0
$+\varepsilon$[0 1 $\bar{1}$]	$\frac{1}{2}$	$-\frac{1}{2} - 2\varepsilon$	$-\frac{1}{2} + 2\varepsilon$	-2ε	2ε	4ε	2ε	-2ε
$+\varepsilon$[1 1 1]	$\frac{1}{2} + 3\varepsilon$	$-\frac{1}{2}$	$-\frac{1}{2}$	3ε	3ε	0	3ε	3ε
$+\varepsilon$[$\bar{2}$ 1 1]	$\frac{1}{2}$	$-\frac{1}{2} - 6\varepsilon$	$-\frac{1}{2} - 6\varepsilon$	6ε	6ε	0	-6ε	-6ε
$+\varepsilon$[0 1 1]	$\frac{1}{2} + 2\varepsilon$	$-\frac{1}{2} - 2\varepsilon$	$-\frac{1}{2} - 2\varepsilon$	4ε	4ε	0	0	0
$\frac{1}{6}$[0 1 1]	$\frac{1}{3}$	$-\frac{1}{3}$	$-\frac{1}{3}$	$-\frac{1}{3}$	$-\frac{1}{3}$	0	0	0

drawn for a pure shear of the type ε[1 1 1]. Any linear combination of these two vectors also does not describe an adequate character for the 3 1 1 α-fringes. A dilatation of the type ε[$\bar{2}$ 1 1] results in a similar contrast for all 3 1 1 reflections. Finally this table shows that only an adequate combination of the magnitudes ε along [1 1 1] and [$\bar{2}$ 1 1] results in an extinction of both 3 1 $\bar{1}$ and 3 $\bar{1}$ 1 contrasts. This is given in the fifth line of Table I, and corresponds to a vector $\boldsymbol{R}_I = \frac{1}{4}$[0 1 1] + ε[0 1 1]. The magnitude ε will be estimated on the basis of α-fringe calculation. This vector is situated between the two extreme values, $\frac{1}{4}$[0 1 1] and $\frac{1}{6}$[0 1 1]. A deviation of the [0 1 1] direction is possible, but it is in any case of a very low magnitude, as it is deduced from the good extinctions in the reflections 3 1 $\bar{1}$ and 3 $\bar{1}$ 1.

6. Detailed characteristics of α-fringes

Fringe profiles have been calculated for different reflections observed in silicon corresponding to experimental conditions. The expressions of intensities developed in three terms ($I_{T,S} = I^1_{T,S} + I^2_{T,S} + I^3_{T,S}$) for α-fringes according to Gevers *et al.* [9] have been chosen. The experimental constants corresponding to a 200 kV accelerating voltage are the following:

$$\xi_{111} = 78\,\text{nm}; \quad \xi_{311} = 169\,\text{nm};$$

$$\xi_{220} = 96\,\text{nm}; \quad (\xi/\xi')_{111} = 0.01;$$

$$(\xi/\xi')_{311} = 0.02; \quad (\xi/\xi')_{220} = 0.013;$$

z_{o111} from 8 to 12 ξ_{111}; z_{o311} from 4 to 6 ξ_{311};

z_{o220} from 8 to 10 ξ_{220}

The anomalous absorption coefficients, ξ_g/ξ'_g, have been calculated according to Humphreys *et al.* [10].

Due to the particularly low value of the anomalous absorption coefficient, it is observed that the calculated fringe systems are not characteristic of the so-called "thick foil contrast". The main characteristics are as follows.

1. There is a pseudo periodicity for the fringe systems of ξ_g; three typical cases are considered:

$$z_o = N\xi_g, \quad z_o = (N + \tfrac{1}{2})\xi_g,$$

$$z_o = (N \pm \tfrac{1}{4})\xi_g \quad (N = \text{integer})$$

2. For any α value and any z_o value, a fringe system for $s = 0$ is similar to a fringe system for a small s value of a crystal with a slightly lower z_o value.

3. $\alpha = 180°$ fringes show always fringe systems with a periodicity $\xi_g/2$ even if $s \neq 0$.

4. $\alpha > 120°$ fringes show always a fringe periodicity of $\xi_g/2$ with alternating subsidiary maxima; more details are given below.

5. Fringe systems for lower α values have the well known characteristics of $\alpha \neq 180°$ fringes for "thick" crystals.

Fig. 1 shows an α-fringes image of a ($\bar{2}$ 1 1) twin boundary taken in the 1 1 1 reflection, and Fig. 2 the same twin boundary observed in the 2 0 $\bar{2}$ reflection. The contrast of the image in Fig. 1, as well as the dedoubled fringe system, suggests a high α value, close to 180°. Fig. 3 is another contrast of the same area, taken with the $\bar{1}$ 3 1 reflection for which a low α value is assumed. The same boundary is out of contrast in

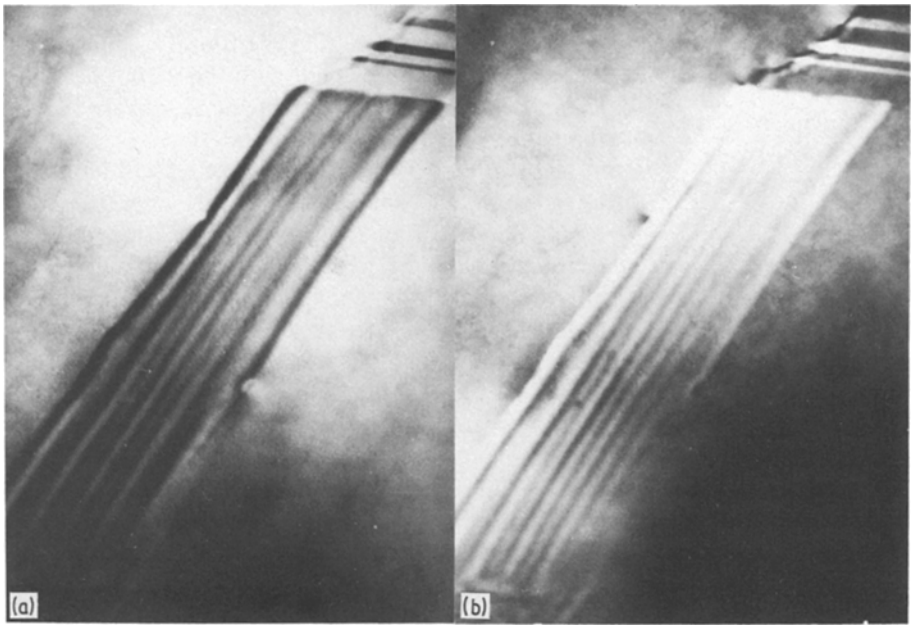

Figure 3 Same twin boundary as in Figs 1 and 2 observed in the $\bar{1}$ 3 1 reflection and showing a fringe system typical of a low α value. (a) bright field in $\bar{1}$ 3 1, (b) dark field in 1 $\bar{3}$ $\bar{1}$.

TABLE II Different α-values for different magnitudes of the translation between the two extreme values of $\frac{1}{4}[0\,1\,1]$ and $\frac{1}{6}[0\,1\,1]$

n	4	4.24	4.5	4.8	5.14	5.54	6
$\alpha_{1\,1\,1}$	180°	170°	160°	150°	140°	130°	120°
$\alpha_{\bar{1}\,3\,1}$	0°	20°	40°	60°	80°	100°	120°

the $3\,\bar{1}\,1$ and $3\,1\,\bar{1}$ reflections. A displacement vector of the type $\boldsymbol{R}_1 = 1/n\,[0\,1\,1]$ is suggested with $4 \leqslant n \leqslant 6$. Alpha fringe profiles have been calculated for seven values of n in this interval. They correspond to the α values for the reflections $1\,1\,1$ and $\bar{1}\,3\,1$ given in Table II.

These profiles have been compared with the micrographs of Figs 1 and 3. Figs 4 and 5 show the BF and DF profiles which best correspond to the observations. The α values are the following:

$$\alpha_{1\,1\,1} = 150° \text{ associated with } \alpha_{\bar{1}\,3\,1} = 60°$$

$$\alpha_{1\,1\,1} = 140° \text{ associated with } \alpha_{\bar{1}\,3\,1} = 80°$$

$$\alpha_{1\,1\,1} = 130° \text{ associated with } \alpha_{\bar{1}\,3\,1} = 100°$$

They correspond to $z_o = 9\xi_{1\,1\,1}$ to $9.5\xi_{1\,1\,1}$ and $z_o = 5\xi_{\bar{1}\,3\,1}$ to $5.5\xi_{\bar{1}\,3\,1}$.

The characterization has been based on the following criteria.

1. The value of n is most sensitive on the intensities of $\alpha_{\bar{1}\,3\,1}$-fringes; therefore the fringe profiles calculated for $\alpha_{\bar{1}\,3\,1} = 60°$, 80° and 100° and for $z_o = 5\xi_g$, $5.25\xi_g$ and $5.5\xi_g$ (Fig. 5) have been compared with the observed image, taking the calculated $\alpha_{1\,1\,1} = 150°$ (Fig. 4), 140° and 130° profiles, as an internal calibration of the magnitude of the contrast.

2. The detailed characteristics of the finge profiles, $\alpha_{1\,1\,1}$, have then been compared with the observations:

(i) in BF, for $z_o = 9\xi_g$, i.e. in a bright background (BG), the dedoubled bright fringes are of equal intensity, while the dedoubled dark fringes have an alternating more dark and less dark intensity;

(ii) in DF, for $z_o = 9\xi_g$, i.e. in a dark BG, the dedoubled dark fringes are of equal intensity, while the dedoubled bright fringes have an alternating more bright and less bright intensity;

(iii) similar properties are observed for $z_o = 9.5\xi_g$, where the roles of the BF and DF are reversed;

(iv) an intermediate situation is observed for $z_o = 9.25\xi_g$;

(v) BF and DF are always complementary.

3. The fringe systems for the reflection $1\,1\,1$ do not correspond to $\alpha = 180°$, otherwise all subsidiary maxima and minima should be of equal intensities.

From these observations it is deduced that a reasonable value for n is around 4.8 or 5.14. These values are not related to the structure, therefore a good approximation of the rigid body translation is:

$$\boldsymbol{R}_1 \cong \tfrac{1}{5}[0\,1\,1]_A$$

This vector corresponds in crystal B to $\boldsymbol{R}_1 \cong \frac{1}{15}[4\,1\,1]_B$. The facets presenting the $\boldsymbol{R}_2$ translation have the following vector:

$$\boldsymbol{R}_2 \cong \tfrac{1}{5}[0\,1\,1]_B = \tfrac{1}{15}[4\,1\,1]_A$$

These vectors describe correctly all the contrasts

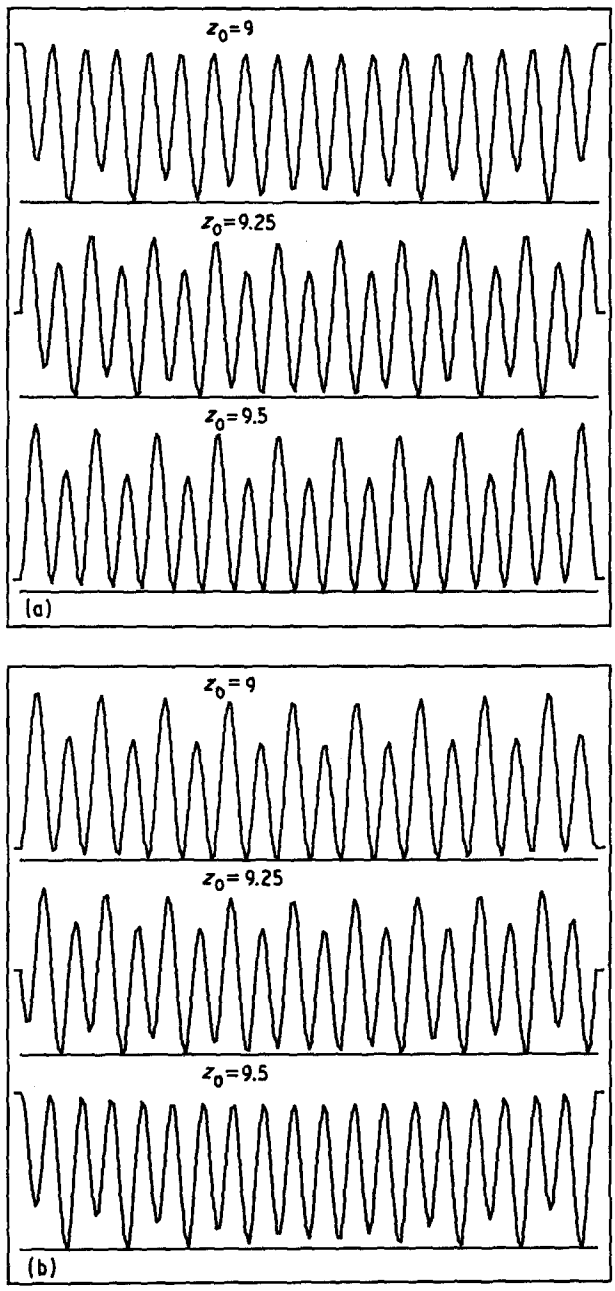

Figure 4 Calculated α-fringe profiles for a stacking fault in silicon in the $1\,1\,1$ reflection ($\xi_g/\xi_g' = 0.01$) for $\alpha = 150°$, $s = 0$. (a) bright field, (b) corresponding dark field.

observed in the $1\,1\,1$ and in the four $3\,1\,1$ reflections. They are also in agreement with the $2\,2\,0$ reflections. The observed $2\,0\,\bar{2}$ contrast of Fig. 2 corresponds to the fringe profile given in Fig. 6.

The contrast of the dislocations present along the intersection line between the $(1\,1\,1)$ and the $(\bar{2}\,1\,1)$ facets has been analysed. No dislocation contrast characterized by $\boldsymbol{g} \cdot \boldsymbol{b} = 1$ has been detected, although the strain field contrast is clearly visible for the $1\,1\,1$ reflections. This indicates that the dislocation contrast is compatible with $\boldsymbol{b} = \frac{1}{5}[0\,1\,1]$.

7. Influence of other reflections

An extreme variability of the fringe contrasts is observed in silicon, which is at the origin of the uncertain determination of the rigid body translation. This is experienced even for so-called clear "two beam" contrasts. Therefore images have been taken for the same $\bar{1}\,3\,1$ reflection, systematically tilting the crystal

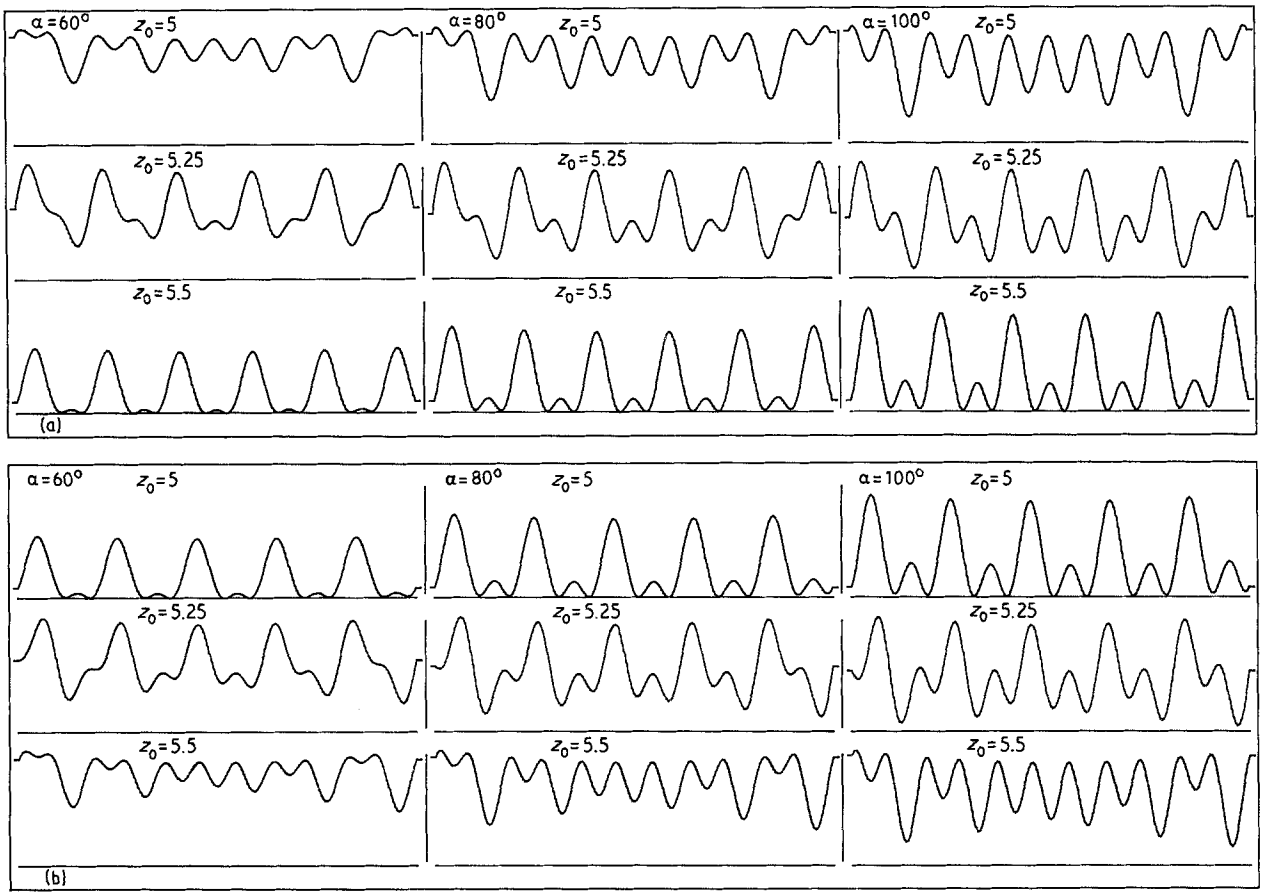

Figure 5 Calculated α-fringe profiles for a stacking fault in silicon in the $\bar{1}\,3\,1$ reflection ($\xi_g/\xi'_g = 0.02$) for $s = 0$. (a) bright field, (b) corresponding dark field.

along the $[\bar{1}\,3\,1]$ axis and carefully avoiding the clear multiple beam diffraction conditions. It has been possible, in these conditions, to achieve a clear determination of the best condition for an unambiguous two beam contrast. This systematic search is important for the determination of the extinction condition, but it is also important for a clear determination of an $\alpha = 60°$ fringe system. Finally, for the contrasts for high α values, this multiple beam influence is less sensitive.

8. Conclusion

The rigid body translation $\boldsymbol{R}_1 \cong \frac{1}{5}[0\,1\,1]$ is rather unexpected since it is in contradiction with all the symmetric atomic models of the $(\bar{2}\,1\,1)$ twin boundary which were at first proposed. On the other hand, it is in agreement with the existence of two different translations, crystallographically equivalent, according to the observations. From the models proposed in the literature and based on energetic simulation, one model meets all the conditions deduced from electron microscopic observations; it is the model presented in Fig. 2b, b_1 of Papon and Petit [8], and reproduced in Fig. 7. The "sticks and balls" model is in agreement with a rigid body translation of $\boldsymbol{R}_1 \cong \frac{1}{5}[0\,1\,1]$; it is also in agreement with the $[0\,1\,1]$ periodicity observed by other authors [7] in electron diffraction. This model is

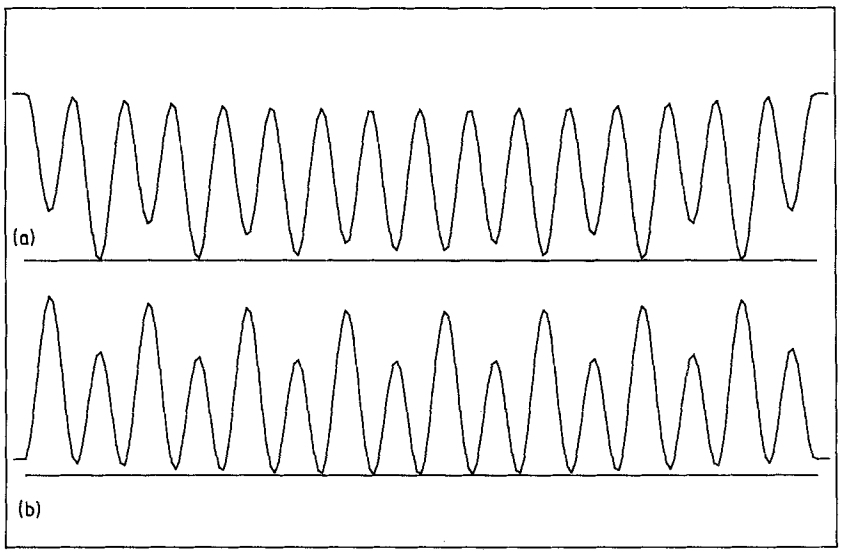

Figure 6 Calculated α-fringe profiles for a stacking fault in silicon in the $2\,0\,\bar{2}$ reflection ($\xi_g/\xi'_g = 0.013$) for $\alpha = 150°$, $z_0 = 8\xi_g$ and $s = 0$. (a) bright field, (b) corresponding dark field.

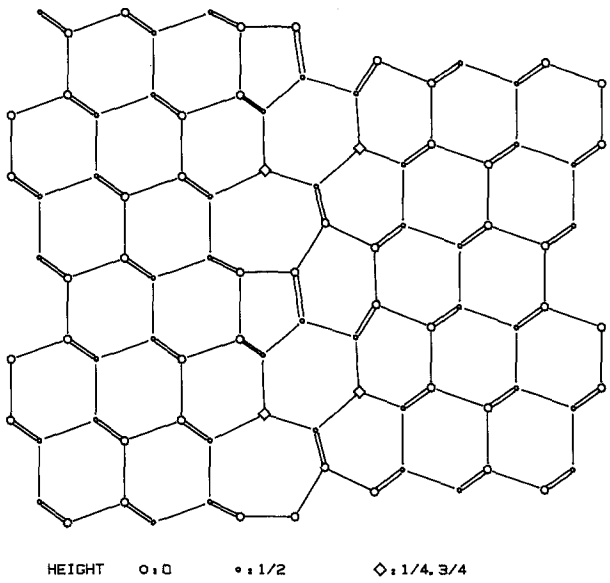

Figure 7 Model of the ($\bar{2}$ 1 1) twin boundary in silicon as proposed by Papon and Petit [8] and showing a rigid body translation in agreement with the observed contrasts.

characterized by the absence of dangling bonds and by a moderate perturbation of the bonds in direction and length. It is therefore concluded that α-fringe contrasts support the existence of this model.

Acknowledgements

The authors wish to thank Dr D. Helmreich of Heliotronic GmbH for the provision of silicon wafers. This work has been partially supported by the Greek Ministry of Research and Technology.

References

1. D. VLACHAVAS and R. C. POND, in "Microscopy of Semiconducting Materials" (International Physics Conference Series No. 60, Institute of Physics, London, 1981) p. 159.
2. C. FONTAINE and D. A. SMITH, *Appl. Phys. Lett.* **40** (1982) 153.
3. M. D. VAUDIN, B. CUNNINGHAM and D. G. AST, *Scripta Met.* **17** (1983) 191.
4. R. C. POND, D. J. BACON and A. M. BASTAWEESY, in"Microscopy of Semiconducting Materials" (International Physics Conference Series No. 67, Institute of Physics, London, 1983) p. 253.
5. A. M. PAPON, M. PETIT and J. J. BACMANN, *Phil. Mag.* **49** (1984) 573.
6. C. D'ANTERROCHES and A. BOURRET, *Phil. Mag.* **49** (1984) 783.
7. A. BOURRET, in "Proceedings of the International School of Materials Science and Technology", edited by G. Harbeke (Springer-Verlag, Berlin, 1984) p. 2.
8. A. M. PAPON and M. PETIT, *Scripta Met.* **19** (1985) 391.
9. R. GEVERS, J. VAN LANDUYT and S. AMELINCKX, *Phys. Stat. Sol.* **11** (1965) 689.
10. C. J. HUMPHREYS and P. B. HIRSCH, *Phil. Mag.* **18** (1968) 115.

Received 14 November 1985
and accepted 10 January 1986